Care and Use Committee at Juntendo University and were conducted in accordance with the U.S. National Institutes of Health Guide for the Care and Use of Laboratory Animals.

## Vectors

A replication-deficient vector (human AdV, serotype 5) was used to encode the green fluorescent protein (GFP) driven by the cytomegalovirus (CMV) promoter. The virus was designated AD5.CMV-GFP ($3 \times 10^{11}$pfu/ml). The E1 and E3 regions were deleted. The vectors were purchased from Arist Company, Osaka, Japan. Viral suspensions in 10 mM Tris-HCl, pH 7.5, 1 mM $MgCl_2$, and 10% glycerol were kept at –80°C until thawed for use.

The plasmid DNA pAAV-MCS (CMV promoter; Stratagene, La Jolla, CA, USA) carrying the *GFP* gene was constructed as reported previously (11). The plasmid DNA pAAV-GFP was cotransfected with plasmids pHelper and Pack2/1 into HEK-293 cells using the standard calcium phosphate method (12). After 48 hours, the cells were harvested, and crude rAAV vector (serotype 1) solutions were obtained by repeated freeze-thaw cycles. After ammonium sulfate precipitation, the virus particles were dissolved in phosphate-buffered saline (PBS) and applied to an OptiSeal centrifugation tube (Beckman Coulter, Fullerton, CA, USA). After overlaying with an OptiPrep solution (Axis-Shield PoC, Oslo, Norway), the tube was processed with a Gradient Master (BioCpmp Instruments, Fredericton, NB, Canada) to prepare the gradient layer of the OptiPrep. The tube was then ultracentrifuged at 13,000 r.p.m. for 18.5 hours. The fractions containing high-titer rAAV vectors were collected and used for injection into animals. The number of rAAV genome copies was semiquantified using polymerase chain reaction (PCR) within the CMV promoter region using primers 5'-GACGTCAATAATGACGTATG-3' and 5'-GGTAATAGCGATGACTAATACG-3'. The final titer was $1.4 \times 10^{13}$ vp/ml.

To compare the infectious efficiency of the 2 vectors, the same volume (0.5 μl) of AdV-GFP and AAV-GFP from the same lots used in the present cochlear injection were administered in 60-mm dish with confluent HEK293 cells and observed in 24 hours after the infection.

## Surgical Procedures

C57BL/6 male mice were anesthetized with ketamine (100 mg/kg) and xylazine (4 mg/kg) by intraperitoneal injection. Glass capillaries (Drummond Scientific, Broomall, PA, USA) were drawn with a PB-7 pipette puller (Narishige, Tokyo, Japan) to achieve an approximately 10-μm outer tip diameter. A polyethylene tube (Atom Medical, Saitama, Japan) was connected to the glass micropipette. After making a left postauricular incision, the vector was injected following either of the 2 routes.

Round window approach: for injection via the round window, the left otic bulla was opened, and the glass micropipette was inserted into the round window up to the scala tympani, and the vectors were injected using the micropipette. The injection volume of the viral vector was regulated to approximately 0.1 μl/min for 5 minutes using a syringe connected to the polyethylene tube. To allow the vector to spread throughout and stabilize in the inner ear, the glass micropipette was left in place for 1 minute after the injection. The opening region of the otic bulla was sealed with connective tissue.

Semicircular canal approach: for injection via canalostomy, after anesthesia, the posterior and lateral semicircular canals were identified, and a small hole was made in each canal. Next, the glass pipette was inserted into the hole of the posterior semicircular canal, and the vectors were injected in the same manner as with the round window approach.

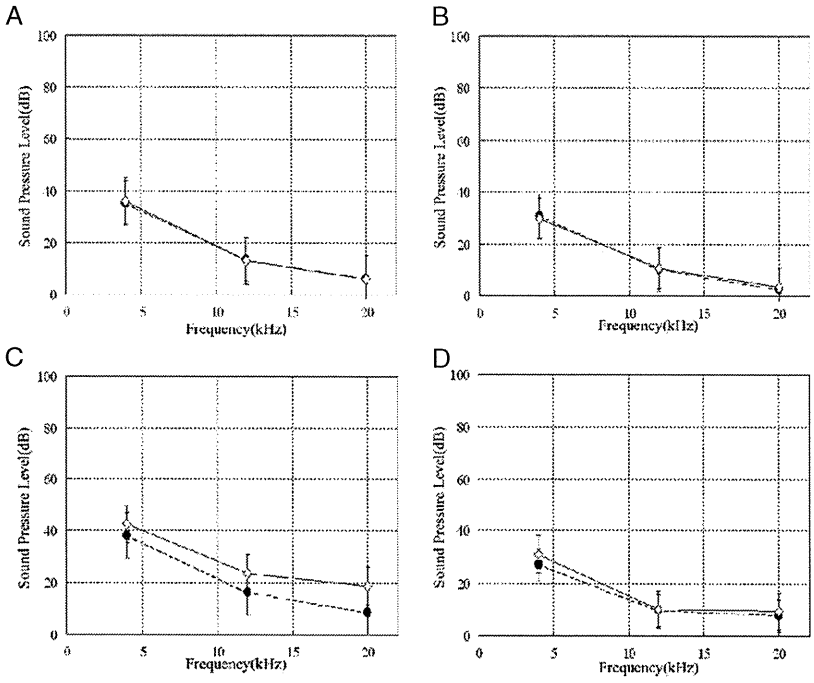


**FIG. 1.** Hearing results at 14 days after virus vector injection. The ABR thresholds of postoperation (*hollow squares*) did not differ from the preoperative results (*solid circles*) of AAV injection via the round window (*A*) and via canalostomy (*B*) and the AdV injection via canalostomy (*D*). At AdV injection via the round window, statistical significance was seen at 20 kHz(*C*). (*$p < 0.05$).

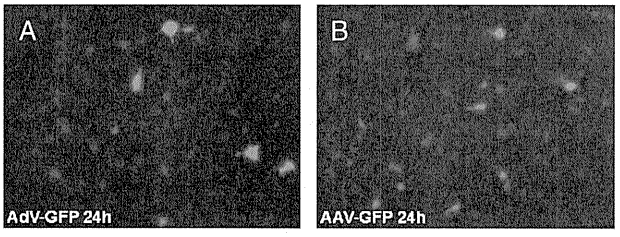


**FIG. 2.** The same volume (0.5 μl) of AdV-GFP (*A*) and AAV-GFP (*B*) from the same lots used in the present cochlear injection were administrated in 60-mm dish with confluent HEK293 cells and observed in 24 hours after the infection. GFP signals showed approximately same infection rates. Images were represented by GFP fluorescent overlaid on phase contrast image.

### Measurements of Auditory Brainstem Response

To assess the safety of the gene transfer strategy, we assessed the auditory brainstem response (ABR) preoperatively and 14 days after the operation at the virus-injected ear (left side). ABR measurements were performed as previously reported in our laboratory (13). Thresholds were determined for frequencies of 4, 12, and 20 kHz from a set of responses at various intensities with 5-dB intervals, and the electrical signals were more than 512 repetitions.

### Assessment of Vestibular Function

We assessed the vestibular function by observation of the head tilt, reaching response, and swimming test at 14 days after operation. For the reaching response, the mouse was held by the tail above a flat surface, and it was noted whether the forepaws were stretched out to make contact with the surface. For the swimming test, the animals were placed in a container filled with 30 cm of comfortably warm water for no longer than 60 seconds.

### Sample Preparation, Histology, and Immunohistochemical Analysis

At 14 days after injection, the mice were anesthetized and perfused intracardially with PBS, followed by 4% paraformaldehyde (PFA) in phosphate buffer. The whole inner ear structures were excised and fixed with PFA and then decalcified in 0.12M ethylenediamine tetra-acetic acid. Specimens were cryoprotected in 30% sucrose in PBS, embedded, frozen, and sectioned at 10 μm. Immunofluorescence analysis was performed as previously reported (10) using anti-GFP antibodies, rhodamine-phalloidin, and 4'6-diamidino-2-phenylindole (DAPI). Images of sections were captured with a Carl Zeiss Axioplan 2 microscope (Carl Zeiss, Oberkochen, Germany), KEYENCE VB-G25 (KEYENCE, Osaka, Japan), and Carl Zeiss LSM510 META (Carl Zeiss, Oberkochen, Germany).

### Data Analysis

Statistical analyses were performed using Student's *t*-test for the ABR data in StatMate IV for Windows. Differences were considered to be significant if $p < 0.05$.

## RESULTS

### Functional Evaluation

The ABR thresholds at frequencies of 4, 12, and 20 kHz are shown in Figure 1. The ABR thresholds 14 days after virus vector injection did not differ from the preoperative results in the rAAV injection (Fig. 1, A and B) and AdV injection via canalostomy groups (Fig. 1D). With AdV injection via the round window (Fig. 1C), the ABR threshold at 20 kHz was significantly elevated postoperatively (Fig. 1C) ($*p < 0.05$). For vehicle control, a sham treatment using sterile normal saline through the round window or semicircular canal had been done without hearing loss (data not shown).

No abnormalities were observed in the vestibular functional tests (head tilt, reaching response, and swimming test) in any animal 14 days after the operation.

### The Infectious Efficiency of the 2 Vectors

GFP signals showed approximately same infection rates, suggesting that these 2 lots of virus had the same titer level. Images were represented by GFP fluorescent overlaid on phase contrast image (Fig. 2).

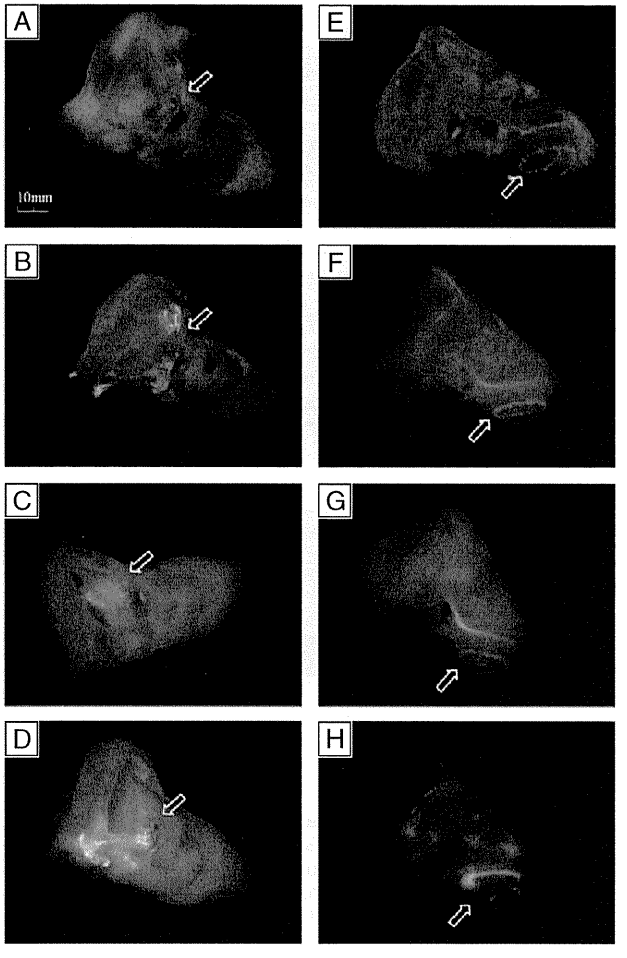


**FIG. 3.** Photomicrographs of whole inner ear images after dissection with a fluorescence stereoscopic microscope. AAV injected inner ear via the round window (*A, E*), AAV injected via canalostomy (*B, F*), AdV injected via the round window (*C, G*), and AdV injected via canalostomy (*D, H*).

### Whole Inner Ear Observation

To confirm the infection of the inner ear, we observed the whole inner ear without staining using a fluorescence stereoscopic microscope. GFP signals were observed in the vestibular organs (Fig. 3, A–D) and the cochlea (Fig. 3, E–H) with all the methods.

### Expression of GFP

We observed the immunostained frozen sections of the vestibular organs with a fluorescence microscope to assess the cellular specificity of the transgene expression of the virus vectors and the numbers of infected cells. No pathologic changes were observed in the vestibular organs. GFP expression could be seen in vestibular hair cells (arrowheads), supporting cells (white arrows), and fibrocytes (outlined arrows) in the inner ear tissue after rAAV injection via the round window (n = 4; Fig. 4, A and B). After rAAV injection via canalostomy, the expression of GFP also was seen in hair cells and supporting cells in the ampulla and utricule, and higher GFP expression was observed in the fibrocytes as compared with the other methods (n = 6; Fig. 4, C and D). After AdV injection via the round window (n = 4; Fig. 4, E and F) and canalostomy (n = 5; Fig. 4, G and H), transgene expression was detected in the ampulla and utricule, corresponding to the hair cells and supporting cells.

For the purpose of identifying GFP-expressing cells, the sections were observed and image-stacked using a confocal laser scanning microscope. After rAAV injection via canalostomy (Fig. 4I) and AdV injection via canalostomy (Fig. 4J), the expression of GFP occurred in supporting cells, organizing a single layer, and hair cells in the shape of flask or column form.

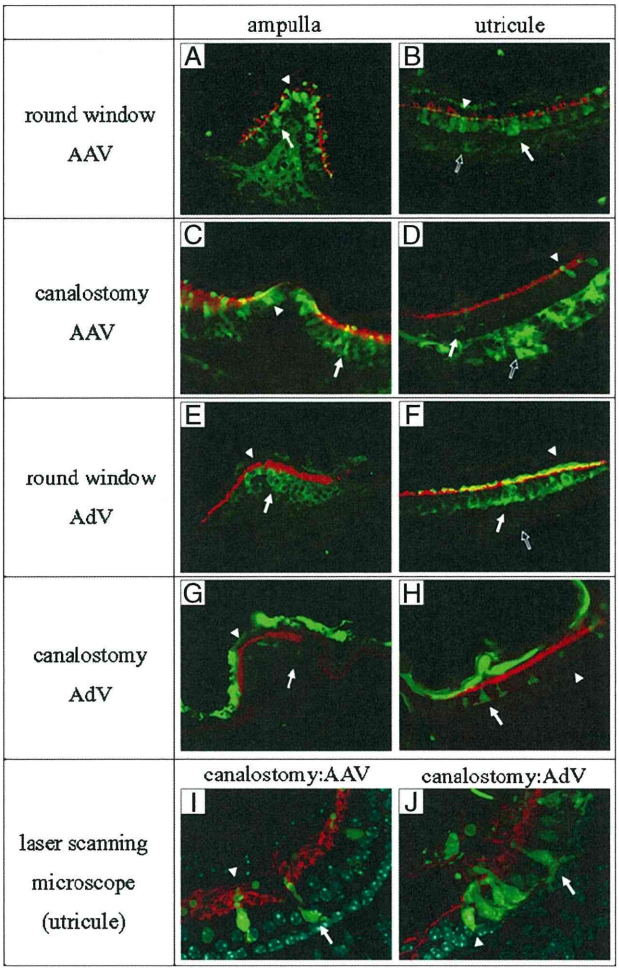


**FIG. 4.** Distribution of GFP expression after the AAV and AdV injection. *A, C, E,* and *G* are ampulla and *B, D, F,* and *H* are utricle. GFP expression could be seen in vestibular hair cells (*arrowheads*), supporting cells (*white arrows*) and fibrocytes (*outlined arrows*) in the inner ear tissue after AAV injection via the round window (*A, B*). Expression of GFP also was seen in hair cells and supporting cells in the ampulla and utricule, and higher GFP expression observed in the fibrocytes compared with the other methods (*C, D*). With AdV injection via the round window (*E, F*) and canalostomy (*G, H*), transgene expression is detected in the ampulla and utricle, including the hair cells and supporting cells. *I* and *J* are the images using a laser scanning microscope. GFP expressions were observed in vestibular hair cells (*arrowheads*) and supporting cells (*white arrows*) with the methods of AAV injection via canalostomy (*I*) and AdV injection via canalostomy (*J*).

**TABLE 1.** *Expression of green fluorescent protein in the vestibular organ*

| | Ampulla | | Utricule | | |
|---|---|---|---|---|---|
| | HC | SC | HC | SC | Fibrocyte |
| AAV-RW injection | ++ | + | ++ | + | + |
| AAV-canalostomy | ++ | ++ | + | + | ++ |
| AdV-RW injection | + | + | + | + | + |
| AdV-canalostomy | + | + | + | + | + |

The number of infected cells in one section is 0 (−), 1~5 (+), and 6~10 (++).

HC indicates hair cell; RW injection, transgene via the round window membrane; SC, supporting cell.

### Comparison of the Number of the Infected Cells by Injection Method

We assessed the cellular specificity by counting the numbers of cells expressing GFP (Table 1). In the hair cells in the ampulla, there were more transfected cells by rAAV injection than by AdV injection. In the supporting cells of the ampulla, the rAAV injection by canalostomy showed the most cells with GFP expression. In the utricule, rAAV injection via the round window showed the most cells with GFP expression of all methods. For vestibular fibrocytes, rAAV injection by canalostomy showed the most transfected cells.

## DISCUSSION

The present study is the first report comparing the gene expression at the vestibule between round window and canalostomy approaches. Most of our methods were shown to be safe in terms of hearing function and vestibular function because no ABR threshold shift or balance

abnormality was observed in our study. Especially, the strategy to inject the virus in the ear by canalostomy has no risk of causing hearing impairment because of the surgical manipulation. In the comparison of the number of transfected cells by the injection methods, rAAV injection by canalostomy was demonstrated to have the most and was safe for transgene infection into the vestibular hair cells and other functional cells in the vestibule.

At present, AdV vectors are commonly used in animal experiments of gene therapy for the inner ear. Staecker et al. (4) demonstrated that math1 gene transfer using AdV results in vestibular hair cell regeneration and recovery of the balance function. Moreover, Pfannenstiel et al. (5) demonstrated that bcl-2 gene transfer using AdV preserved vestibular hair cells after exposure to aminoglycosides. The expression time of AAV may be more useful for therapeutics requiring long time expression, whereas AdV would be used for short-term treatments (6).

Kawamoto et al. (9) reported that no significant ABR threshold shift appeared after the injection of AdV vectors into the mouse inner ear. On the other hand, our study showed that the injection of AdV vectors via the round window significantly elevated the ABR threshold postoperatively at 20 kHz. AdV vectors may cause an inflammatory response in the inner ear because higher titers of AdV and rAAV were used in the present study than in the reports by Kawamoto et al.

Because the titer of rAAV was different from that of AdV, we could not compare the efficiency of AdV with AAV. Although the ABR threshold was significantly elevated after the AdV injection via the round window, it was not elevated after the AAV injection. In addition, the infected hair cells, supporting cells and fibrocytes of the ampulla by AAV injection were greater in number than those by AdV. Thus, rAAV vectors are more suitable than AdV for the purpose of gene therapy to the vestibule.

With AdV injection via a canalostomy, transgene expression was reported to be limited to the perilymphatic space (9). In our study, both AdV and rAAV injection via canalostomy showed transgene expression in vestibular hair cells and supporting cells. Our results differ from those of a previous study (9) and may be explained by the use of the fine glass capillary, which maintains the structure and function of the membraneous labyrinth.

Our noninvasive and highly efficient transfection method could enable transgene infection into the vestibule and may have the potential to repair balance disorders in human in the future.

## REFERENCES


1. Tsuji K, Velazquez-Villasenor L, Rauch SD, Glynn RJ, Wall C 3rd, Merchant SN. Temporal bone studies of the human peripheral vestibular system. Meniere's disease. *Ann Otol Rhinol Laryngol Suppl* 2000;181:26–31.
2. Tsuji K, Velazquez-Villasenor L, Rauch SD, Glynn RJ, Wall C 3rd, Merchant SN. Temporal bone studies of the human peripheral vestibular system. Aminoglycoside ototoxicity. *Ann Otol Rhinol Laryngol Suppl* 2000;181:20–5.
3. Proctor L, Perlman H, Lindsay J, Matz G. Acute vestibular paralysis in herpes zoster oticus. *Ann Otol Rhinol Laryngol* 1979;88:303–10.
4. Staecker H, Praetorius M, Baker K, Brough DE. Vestibular hair cell regeneration and restoration of balance function induced by math1 gene transfer. *Otol Neurotol* 2007;28:223–31.
5. Pfannenstiel SC, Praetorius M, Plinkert PK, Brough DE, Staecker H. Bcl-2 gene therapy prevents aminoglycoside-induced degeneration of auditory and vestibular hair cells. *Audiol Neurootol* 2009;14:254–66.
6. Berkner KL. Expression of heterologous sequences in adenoviral vectors. *Curr Top Microbiol Immunol* 1992;158:39–66.
7. Kaplitt MG, Xiao X, Samulski RJ, et al. Long-term gene transfer in porcine myocardium after coronary infusion of an adeno-associated virus vector. *Ann Thorac Surg* 1996;62:1669–76.
8. Lalwani AK, Walsh BJ, Carvalho GJ, Muzyczka N, Mhatre AN. Expression of adeno-associated virus integrated transgene within the mammalian vestibular organs. *Am J Otol* 1998;19:390–5.
9. Kawamoto K, Oh SH, Kanzaki S, Brown N, Raphael Y. The functional and structural outcome of inner ear gene transfer via the vestibular and cochlear fluids in mice. *Mol Ther* 2001;4:575–85.
10. Iizuka T, Kanzaki S, Mochizuki H, et al. Noninvasive in vivo delivery of transgene via adeno-associated virus into supporting cells of the neonatal mouse cochlea. *Hum Gene Ther* 2008;19:384–90.
11. Yamada M, Iwatsubo T, Mizuno Y, Mochizuki H. Overexpression of alpha-synuclein in rat substantia nigra results in loss of dopaminergic neurons, phosphorylation of alpha-synuclein and activation of caspase-9: resemblance to pathogenetic changes in Parkinson's disease. *J Neurochem* 2004;91:451–61.
12. Sambrook JRD, Russel DW. Calcium-phosphate-mediated transfection of eukaryotic cells with plasmid DNAs. In: Irwin N, Janssen KA, eds. *Molecular Cloning: A Laboratory Manual.* New York, NY: Cold Spring Harbor Laboratory Press, 2001:16.14–16.20.
13. Inoshita A, Iizuka T, Okamura HO, et al. Postnatal development of the organ of Corti in dominant-negative Gjb2 transgenic mice. *Neuroscience* 2008;156:1039–47.

III. 臨床応用の進歩

# 多能性幹細胞を用いた遺伝性難聴に対する内耳細胞治療法の開発

神谷和作　池田勝久

**Inner ear cell therapy for hereditary deafness with multipotent stem cells**

Kazusaku Kamiya, Katsuhisa Ikeda
Department of Otorhinolaryngology, Juntendo University School of Medicine

**Abstract**

Congenital deafness affects about 1 in 1,000 children and the half of them have genetic background such as connexin26 gene mutation. The strategy to rescue such hereditary deafness has not been developed yet. Inner ear cell therapy for hereditary deafness has been studied using some laboratory animals and multipotent stem cells, although the successful reports for the hearing recovery accompanied with supplementation of the normal functional cells followed by tissue repair and recovery of the cellular/molecular functions have been still few. To succeed in hearing recovery by inner ear cell therapy, appropriate cell type, surgical approach and the stem cell homing system to the niche are thought to be required.

**Key words**: hereditary deafness, mesenchymal stem cell, inner ear, cochlea, connexin26

## はじめに

先天性難聴は1,000出生に1人と高頻度に発症し聴覚・言語発育障害の極めて高度なQOLの低下をもたらすが，その半数以上は遺伝性と考えられている．遺伝性難聴の原因遺伝子は代表的なコネキシン26遺伝子(connexin26, Cx26, GJB2)をはじめとして多くが同定されている．しかしその根本的治療法は皆無であり，近年では再生医療の遺伝性難聴への応用が大きく期待されている．著者らは蝸牛線維細胞を標的とした感音性難聴モデルへの内耳細胞治療法に成功し，幹細胞導入により感音性難聴の聴力回復が可能であることを実証した[1]．一方でヒト遺伝性難聴の臨床症状に近いとされる遺伝子改変モデルマウスの開発も進めてきた．ヒト非症候性難聴DFN3モデルBrn4欠損マウス(Brn4KO)は遺伝性難聴の遺伝子改変モデルの先駆けとして報告され，蝸牛線維細胞の変性とそれに伴う内リンパ電位(endocochlear potential: EP)と呼ばれる内耳特異的な電位形成のシステムに異常が生じることが初めて発見された(図1)[2]．更に世界で最も高頻度に変異が検出される代表的な難聴遺伝子，コネキシン26(Cx26)遺伝子(*GJB2*)の優性阻害変異型トランスジェニック(Tg)マウス(Cx26Tg)[3]の作製によっても，高頻度に発生する遺伝性難聴に対する分子病態が明らかになってきた．このマウスは生後発達期に

順天堂大学医学部 耳鼻咽喉科学講座

0047-1852/11/¥60/頁/JCOPY

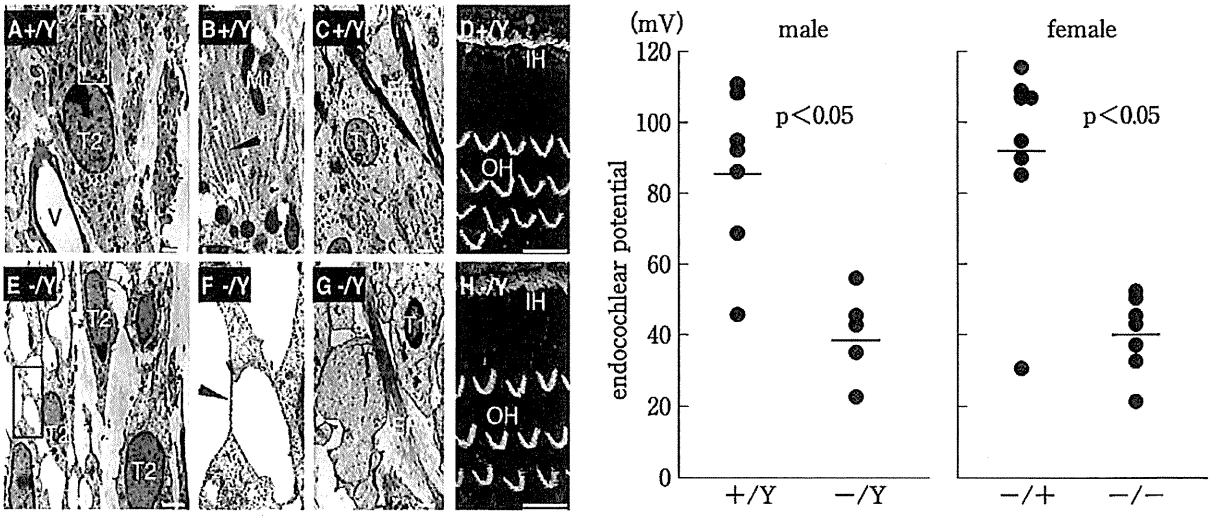


**図1　ヒト遺伝性難聴モデルBrn4遺伝子欠損マウスにおける蝸牛線維細胞変性の発見**(文献[2]より引用)

蝸牛有毛細胞を含むコルチ器に変性がないにもかかわらず(H)，蝸牛線維細胞に変性がみられ(F，矢頭)，その結果蝸牛内リンパ電位が著しく低下する(右グラフ)．→すなわち蝸牛線維細胞を正常細胞に置換することができれば聴力が回復する可能性が非常に高い．

有毛細胞を含む感覚上皮領域であるコルチ器において，コルチトンネルやヌエル腔などの特殊細胞構築(cytoarchitecture)が正常に形成されないという病理的特徴があるが[4]，外有毛細胞を単離すると正常と同等の有毛細胞特有の運動能を示すことが明らかとなり[5]，残存した有毛細胞を活用した細胞治療により，聴力回復の可能性が十分に考えられる．

著者らの研究チームではCx26の内耳特異的欠損マウス(Cx26cKO)を新規開発し，同モデルマウスによる更なる分子病態の解明とそれに応じた細胞治療法の開発を進めている．

## 1. 内耳細胞治療の必要性

遺伝性難聴では一部の患者に人工内耳の有用性も報告されているが，本来の聴覚機能を回復させる根本的治療法はいまだ存在しない．遺伝性難聴の第一次的な原因細胞は有毛細胞以外にも蝸牛線維細胞や支持細胞などであることが明らかとなっている．この多様な異常変異細胞を修復するには，新たな治療戦略として多能性幹細胞を用いた効率的細胞治療法の開発が必要であると考えられる．内耳再生医療の技術開発により，これまで補聴器や人工内耳などの適用で根本的治療が存在しなかった遺伝性難聴患者の日常生活における負担は大幅に減り，細胞が永続的に生着すればその後の手術や投薬の頻度が軽減し，極めて現実的な高度医療への発展が期待できる．

## 2. 内耳への細胞治療とそのアプローチ

近年の内耳再生医療に関する基礎研究分野は，*in vitro*での有毛細胞への分化誘導においては年々進歩している．最近では*in vitro*においてマウス胚性幹(ES)細胞や人工多能性幹(iPS)細胞から聴毛を有する有毛細胞へ分化誘導することも可能となっており[6]，細胞工学的分野では大きな成果が得られている．しかしながらそれらの細胞を移植により内耳組織へ生着させ，同時に機能的補足や組織修復によって聴力回復を誘導する細胞治療の試みは成功例が少なく，引用度の高い論文での報告も少ない．聴力回復を目的とした内耳細胞治療法を開発するためには移植細胞の生着と機能発現を同時に考慮し，内耳の解剖学的特徴および各細胞の生理学的特徴を十分に理解することが重要であると考えられる．

内耳は特殊なリンパ液で満たされた独特な構造をもち，血液-脳関門と同様に‘血液-内耳関

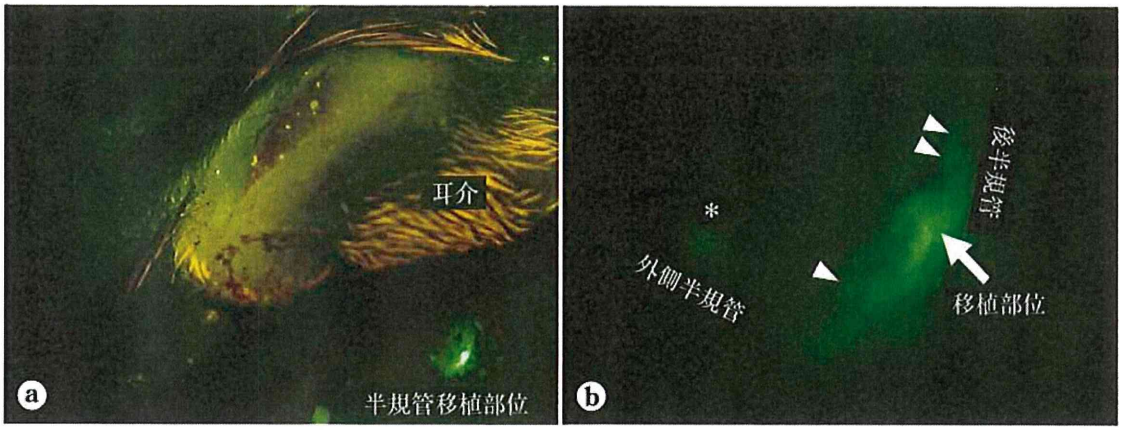


**図2 マウスへの間葉系幹細胞移植2週間後の移植部蛍光実体顕微鏡像**

a. 耳後部切開により半規管を露出し，移植細胞塊が拒絶されずに生着していることを確認．

b. 更に移植部位より播種性に進展し，コロニーを形成(矢頭)．後半規管から外側半規管への移行も確認された(＊)．

門'と呼ばれる血管系を有するため内耳有毛細胞やその周辺細胞への薬物的アプローチが難しい．しかし移動能・多分化能を兼ね備えた幹細胞による内耳細胞治療の方法が確立すれば，難聴の根本的治療への有効なツールになると考えられる．

著者らの初期の検討実験では，蝸牛管付近より細胞液投与を試みた際はどの部位でも手術による永続的な聴力低下がみられ，蝸牛組織には線維化が認められた．著者らはIguchiらの方法[7]を参考にラットの後半規管および外側半規管に小孔を開け[7]，片側から微小チューブを挿入し細胞液の外リンパ腔還流($1\times10^5$ cells/20 $\mu$L×10 min)を行い，良好な結果が得られている．この方法では手術による聴力低下はほとんどみられず，大量の細胞を蝸牛内に導入することができるため，内耳細胞治療に適した投与法であると思われる．著者らは細胞液環流後に骨髄間葉系幹細胞の細胞塊を半規管の小孔に挿入することにより，内液の漏出を防ぎ，細胞生着にも良好な結果を得ている(図2)．

### 3. *in vitro* での内耳有毛細胞作製法の開発

体外で未分化細胞より内耳有毛細胞を作製しようとする試みは数多く行われてきたが，*in vitro* において有毛細胞特異的マーカーを発現させた報告はこれまで複数報告されてきた．それらを発展させ，遺伝子発現だけではなく特殊な巨大繊毛をもつ内耳有毛細胞に特殊形態を形成させ，最終的には音の振動を感知する機械的刺激受容チャネル(機械電気シグナル変換チャネル：mechanoelectrical transduction(MET) channel)を併せ持つ細胞を作製させる試みがついで行われてきた．2007年にCorwinらの研究チームはニワトリの間葉系細胞から動毛，不動毛をもつ有毛細胞を作製した[6]．次段階として，哺乳類細胞から有毛細胞を *in vitro* で作製する技術が期待されてきた．そして2010年，スタンフォード大学のOshima，Hellerらの研究チームによりマウスのES細胞およびiPS細胞から *in vitro* で内耳有毛細胞を作製する画期的技術が発表され，作製された細胞が音の振動を感知できる有毛細胞特有のMET機能を有することが明らかとなった[8]．これにより内耳有毛細胞を体外で人工的に増殖・分化させることが可能であることが示された．この報告では，未分化細胞から内耳前駆細胞へ，段階的に分化を進めているため，これを応用すればすべての内耳構成細胞への分化能をもつ内耳細胞を *in vitro* にて作製し内耳移植に最適な細胞を選抜することが可能となる．同方法ではES/iPS細胞の浮遊培養後に接着培養を行い分化制御因子としてDkk1，SIS3，IGF-1の添加培養，その後の

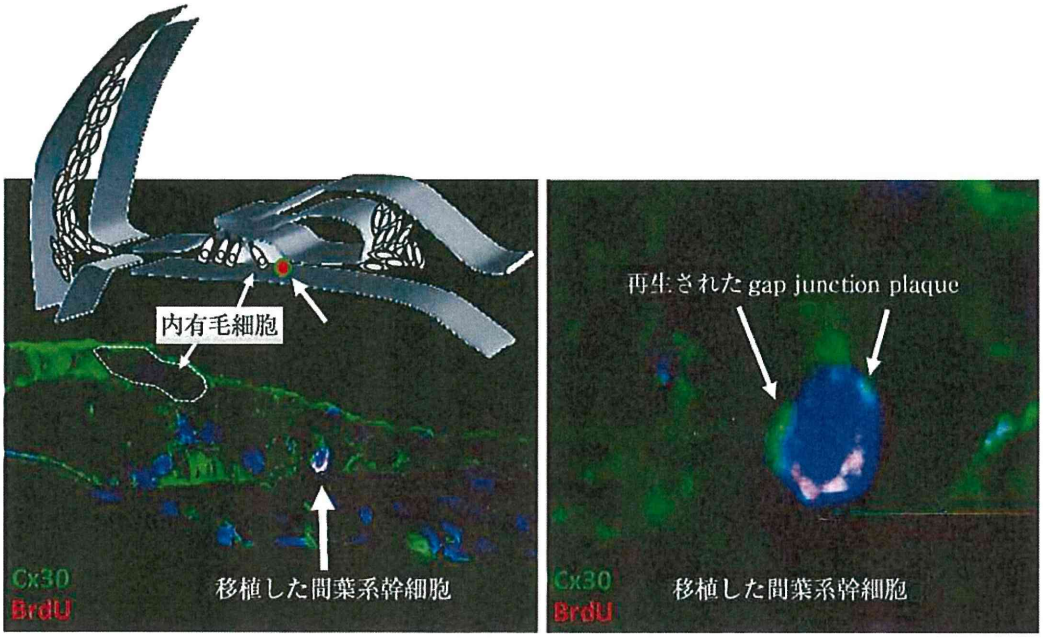


**図3　移植した間葉系幹細胞において再生されたギャップ結合プラーク**
半規管外リンパ液領域より移植され，コルチ器の内有毛細胞近傍に侵入した間葉系幹細胞(左)．同細胞は蝸牛支持細胞の機能構造であるコネキシン複合体で構成されるギャップ結合プラークを形成している(右)．

bFGF 添加後に鶏杯卵形嚢細胞との共培養を行うことで，動毛や機械電気シグナル変換が可能な不動毛をもつ内耳有毛細胞様細胞を得ることを可能としている．

## 4. 蝸牛標的組織への幹細胞の誘導

前述のように体外で内耳細胞を作製する技術は大きく進展しているが，内耳細胞治療において，作製された細胞を蝸牛組織へ直接的に挿入することは蝸牛の構造上困難であり，適切な箇所に幹細胞を導入できる細胞誘導システムが必須であると考えられる．特に有毛細胞やその支持細胞および内リンパ液に接する血管条細胞，蝸牛線維細胞など，適切な箇所に幹細胞を導入し，その微小環境(niche，ニッチ，ニッシェ)に応じて分化させることが必要である．そのためには適切な幹細胞ホーミング(標的組織へ遊走し微小環境に生着)の分子機構を理解し応用することが重要であると考えられる．

マックスプランク研究所の研究チームは，心筋虚血後に骨髄由来間葉系幹細胞が瘢痕層へ効率的にホーミングされるには走化性因子 MCP1 とその受容体 CCR2 およびその下流において細胞遊走を制御している FROUNT による分子経路が重要な役割を担っていることを明らかにした[9]．著者らの研究チームでは，実験的に誘発した蝸牛線維細胞損傷部においても MCP1 が高発現することを発見している(文献[1]および未発表データ)．これを応用し CCR2 を共発現する骨髄間葉系幹細胞株を作製して内耳細胞治療実験に用いることで，良好な細胞誘導効果が得られている．これまで蝸牛線維細胞領域に軽度損傷を与えた難聴動物では蝸牛線維細胞に移植細胞が侵入しており，一部は有毛細胞の近傍の支持細胞領域に侵入し，同領域の主な機能構造であるギャップ結合プラークを形成した(**図3**)．

## おわりに

将来的に内耳細胞治療への活用が期待できる細胞は，患者の骨髄より樹立可能な骨髄間葉系幹細胞，iPS 細胞および ES 細胞由来の内耳前駆細胞などであるが，これらの細胞と適切な幹細胞ホーミングの分子機構を応用し適切な遺伝性難聴モデル動物において方法を選抜することに

より，細胞を補うだけではなく遺伝子変異をもつ異常細胞を正常細胞に置換するという全く新しい観点での方法論を確立できる．この方法論の発展により，将来的には多様な遺伝性難聴患者に対し薬物治療などとは異なる，組織損傷の種類と度合いに対応した低リスクで高い効果をもつ新規難聴治療法の開発が期待できる．

## ■文　献


1) Kamiya K, et al: Mesenchymal stem cell transplantation accelerates hearing recovery through the repair of injured cochlear fibrocytes. Am J Pathol **171**: 214-226, 2007.
2) Minowa O, et al: Altered cochlear fibrocytes in a mouse model of DFN3 nonsyndromic deafness. Science **285**: 1408-1411, 1999.
3) Kudo T, et al: Transgenic expression of a dominant-negative connexin26 causes degeneration of the organ of Corti and non-syndromic deafness. Hum Mol Genet **12**: 995-1004, 2003.
4) Inoshita A, et al: Postnatal development of the organ of Corti in dominant-negative Gjb2 transgenic mice. Neuroscience **156**: 1039-1047, 2008.
5) Minekawa A, et al: Cochlear outer hair cells in a dominant-negative connexin26 mutant mouse preserve non-linear capacitance in spite of impaired distortion product otoacoustic emission. Neuroscience **164**: 1312-1319, 2009.
6) Hu Z, Corwin JT: Inner ear hair cells produced in vitro by a mesenchymal-to-epithelial transition. Proc Natl Acad Sci USA **104**: 16675-16680, 2007.
7) Iguchi F, et al: Surgical techniques for cell transplantation into the mouse cochlea. Acta Otolaryngol Suppl (551): 43-47, 2004.
8) Oshima K, et al: Mechanosensitive hair cell-like cells from embryonic and induced pluripotent stem cells. Cell **141**: 704-716, 2010.
9) Belema-Bedada F, et al: Efficient homing of multipotent adult mesenchymal stem cells depends on FROUNT-mediated clustering of CCR2. Cell Stem Cell **2**: 566-575, 2008.

International Journal of Pediatric Otorhinolaryngology 75 (2011) 211–214

Contents lists available at ScienceDirect

International Journal of Pediatric Otorhinolaryngology

journal homepage: www.elsevier.com/locate/ijporl

# Prevalence of *GJB2* causing recessive profound non-syndromic deafness in Japanese children

Chieri Hayashi [a,*], Manabu Funayama [b], Yuanzhe Li [c], Kazusaku Kamiya [a], Atsushi Kawano [d], Mamoru Suzuki [d], Nobutaka Hattori [b,c], Katsuhisa Ikeda [a]

[a] Department of Otorhinolaryngology, Juntendo University School of Medicine, 2-1-1 Hongo, Bunkyo-ku, Tokyo 113-8421, Japan
[b] Research Institute for Diseases of Old Age, Juntendo University School of Medicine, Japan
[c] Department of Neurology, Juntendo University School of Medicine, Japan
[d] Department of Otorhinolaryngology, Tokyo Medical University School of Medicine, Tokyo, Japan

ARTICLE INFO

*Article history:*
Received 14 June 2010
Received in revised form 18 October 2010
Accepted 2 November 2010
Available online 26 November 2010

*Keywords:*
Congenital deafness
Cochlear implantation
Japanese children
p.P225L
Connexin 26
*GJB2*

ABSTRACT

*Objective:* *GJB2* (gap junction protein, beta 2, 26 kDa: connexin 26) is a gap junction protein gene that has been implicated in many cases of autosomal recessive non-syndromic deafness. Point and deletion mutations in *GJB2* are the most frequent cause of non-syndromic deafness across racial groups. To clarify the relation between profound non-syndromic deafness and *GJB2* mutation in Japanese children, we performed genetic testing for *GJB2*.
*Methods:* We conducted mutation screening employing PCR and direct sequencing for *GJB2* in 126 children who had undergone cochlear implantation with congenital deafness.
*Results:* We detected 10 mutations, including two unreported mutations (p.R32S and p.P225L) in *GJB2*. We identified the highest-frequency mutation (c.235delC: 44.8%) and other nonsense or truncating mutations, as in previous studies. However, in our research, p.R143W, which is one of the missense mutations, may also show an important correlation with severe deafness.
*Conclusion:* Our results suggest that the frequencies of mutations in *GJB2* and *GJB6* deletions differ among cohorts. Thus, our report is an important study of *GJB2* in Japanese children with profound non-syndromic deafness.



## 1. Introduction

People with any degree of sensory impairment may encounter problems such as discrimination within the education system or when looking for work, and a reduced life expectancy. Sensorineural hearing loss (SNHL) is the most common sensory impairment in developed societies [1,2], where one child in 1000 presents at birth with severe or profound deafness [3].

Recent advances in human genetics have indicated that more than half of congenital SNHL cases involve a genetic factor [4]. In 75–80% of genetic cases, SNHL is the result of autosomal recessive inheritance, and both parents have normal hearing [5]. Mutations of *GJB2* are the most frequent cause of autosomal recessive non-syndromic deafness. Indeed, previous studies have shown that *GJB2* mutations account for up to 50% of non-syndromic deafness cases [6]. Hearing-impaired subjects with biallelic *GJB2* mutations range widely but most commonly follow a severe to profound and non-progressive pattern [7–9]. About 100 different *GJB2* mutations have been reported globally [the Connexin-Deafness homepage: http://davinci.crg.es/deafness/], and these mutations show a relatively high local dependence (founder effect). A high prevalence of c.35delG has been found among Caucasians; c.235delC among Eastern Asians, including Japanese [10–13]; c.167delT among Ashkenazi Jews [14]; p.R143W among certain Africans [15]; and p.W24X among Indians [16,17] and European Gypsies [18–20]. Some recent reports have indicated a genotype-phenotype correlation: children with two truncating mutations, such as c.35delG or c.235delC, are profoundly deaf, while children with a truncating and missense mutation, or two missense mutations, show better hearing [9,21,22]. Since improved speech performance after cochlear implantation in early childhood is usually observed in hearing-impaired subjects with *GJB2* mutations [23], the genetic testing of newborn babies will provide useful prognostic information when selecting appropriate treatment for such children.

In the present study, to clarify the frequency and genotype–phenotype correlation of *GJB2* mutations in children with profound non-syndromic deafness, we performed genetic testing for *GJB2* mutations involving 119 Japanese children who had undergone cochlear implantation with congenital deafness.

* Corresponding author. Tel.: +81 3 5802 1229; fax: +81 3 5840 7103.
*E-mail address:* chieri-h@juntendo.ac.jp (C. Hayashi).

0165-5876/$ – see front matter © 2010 Elsevier Ireland Ltd. All rights reserved.
doi:10.1016/j.ijporl.2010.11.001

## 2. Materials and methods

### 2.1. Subjects

We enrolled 119 Japanese children, who were unrelated to each other, with non-syndromic deafness for genetic analysis. Of these, 107 were sporadic cases (with only one affected individual in the family); the remaining 12 patients were autosomal recessive cases (with normal hearing parents and at least two affected children). The study sample consisted of 70 males (58.8%) and 49 females (41.2%). All of their hearing impairment levels were severe (71–95 dB) to profound (>95 dB); impairments were detected between 0 and 3 years old. All children had undergone cochlear implantation at Tokyo Medical University School of Medicine.

All cases underwent otoscopic examination and audiometric testing. Subjective tests of hearing acuity were assessed based on the auditory brain-stem response (ABR) and auditory steady-state response (ASSR) in infants and children. Behavioral observation audiometry (BOA) was used as a subsidiary measure to ABR and ASSR. A detailed history was taken to exclude other possible causes of deafness (such as neonatal complications, bacterial meningitis or other infections, use of ototoxic medication, or head trauma). Extended pedigrees were elicited from each family to exclude interfamilial relations. Temporal bone computed tomography was used in children to exclude any anomalies. The control group was carefully chosen to determine the carrier frequency, and consisted of 150 unrelated individuals with normal hearing.

Informed consent was obtained from the parents or guardians when necessary, and these were approved by the Ethical Committees of Juntendo University School of Medicine.

### 2.2. Genetic analysis

All samples from the children and normal controls were extracted from peripheral blood using the QIAamp DNA Blood Mini Kit (QIAGEN, Germantown, MD, USA). The coding region of *GJB2* was amplified from DNA samples by the polymerase chain reaction (PCR) using the primers *GJB2*-F 5′-GTGTGCATTCGTCTTTTCCAG-3′ and *GJB2*-R 5′-GCGACTGAGCCTTGACA-3′. PCR products were sequenced using the PCR primers and sequence primers *GJB2*-A 5′-CCACGCCAGCGCTCCTAGTG-3′ and *GJB2*-B 5′-GAAGATGCTGCT GCTTGTGTAGG-3′. The sequencing reaction products were electrophoresed on an ABI Prism 310 Analyzer (Applied Biosystems). When no mutation or a single heterozygous mutation in *GJB2* was confirmed, we performed the multiplex PCR assay and direct sequencing for the coding region of *GJB6*. Multiplex PCR was carried out according to the method of Del Castillo et al. [24] to confirm the presence of the del(*GJB6*-D13S1830) and del(*GJB6*-D13S1854) deletions in *GJB6*.

Samples with no mutation or a single heterozygous mutation in *GJB2* and *GJB6* were analyzed for the gene dosage using real-time quantitative PCR (qPCR) to detect exon rearrangements in *GJB2* and *GJB6*. qPCR was performed with TaqMan Gene Expression Assays (Hs00269615_s1 for *GJB2*, and Hs00272726_s1 for *GJB6*, Applied Biosystems) and the 7500 Fast Real-Time PCR System (Applied Biosystems).

We obtained blood samples from the family which had one of two unreported mutations, pP225L, and the unreported one was confirmed as follows. The samples were subjected to mutation screening by PCR and direct sequencing for *GJB2*. The PCR product was subcloned into pCR 2.1 vecto-TOPO by TOPO TA cloning (Invitrogen, Carlsbad, CA, USA), and independent subclones were sequenced employing M13forward (5_-TTGTAAAACGACGGCCAG) and reverse (5_-ACACAGGAAACAGCTATG) primers. The sequence data using in this study have been submitted to the GenBank databases under accession numbers X65361, AB098335, NM_000816, and NM_001037.

### 2.3. Statistical analysis

A *Z*-test was used to calculate the difference in the allele frequency. In all statistical analyses, *P*-values of 0.01 or less were considered significant.

## 3. Results

### 3.1. Mutation screening of GJB2

*GJB2* mutations were found in 45 of the 119 affected individuals, and, of these, 35 patients were homozygous or compound heterozygous (29.4%). *GJB2*-related deafness patients, who had two *GJB2* mutant alleles, were found in 7 of 12 familial cases (58.3%), and there were 28 of 107 sporadic cases (26.2%). Eight mutations, including two unreported ones (p.R32S and p.P225L), were identified in these patients (Table 1). Three mutations were truncating mutations [one was a nonsense mutation (p.Y136X), and two were frameshifts (c.235delC and c.176-191del)]. The remaining five were missense mutations (p.R143W, p.G45E, p.T86R, p.R32S, and p.P225L). Among these mutations, c.235delC was the most frequent. The c.235delC mutation accounted for 52.9% (37 of 70) of the *GJB2*-mutated alleles (Table 1).

We identified 10 subjects who had three or more mutations. All of them had p.G45E and p.Y136X, including one homozygous child. TA cloning and sequencing of subcloned PCR products revealed that all subjects had both mutations in the same allele (data not shown). G45E accompanied with Y136X has been reported as a pathogenic mutation in previous reports, especially in Japanese patients [11,25], although it remains unclear which mutation is more related to the pathogenicity.

We compared the allele frequency for each mutation with that in Ohtsuka's study [25] (Fig. 1). The frequency of c. 235delC and three mutations (p.R143W, p.G45E/Y136X, and c.176-191del) in this study were significantly different from that in Ohtsuka's study ($P < 0.01$). While the p.V37I mutation was reported to be the second most frequent autosomal recessive deafness allele in Asian countries [11,12], the present subjects did not follow this pattern.

In one subject, we identified a missense mutation, p.P225L, which has not previously been reported (Fig. 2). The sister and father of the proband had this mutation, while they showed a normal hearing function. The mother, with a normal hearing function, showed no mutation at this site, while she revealed only heterozygous p.G45E/Y136X mutation as a known pathogenic mutation of *GJB2*. The sequencing results of TA cloning further confirmed the existence of the pP225L nonsense mutation in this patient. We also identified another unreported mutation, p.R32S, in another subject. The patient had p.R32S/p.G45E/Y136X mutations. The amino acid positions of two unreported mutations

**Table 1**
Mutations identified in the Cx26 gene, *GJB2* (NG_008358.1), in child cases of congenital deafness.

| Nucleotide change | Amino acid change | Allele (%) |
|---|---|---|
| c.235delC | p.Leu79CysfsX3 | 37 (52.9) |
| c.427C>T | p.Arg143Trp(p.R143W) | 15 (21.4) |
| c.134G>A/c.408C>A | p.Gly45Glu/p.Tyr136X(p.G45E/Y136X) | 10 (14.3) |
| c.176_191del | p.Gly59AlafsX18 | 4 (5.7) |
| c.257C>G | p.Thr86Arg(p.T86R) | 2 (2.9) |
| c.94C>A | p.Arg32Ser[a](p.R32S) | 1 (1.4) |
| c.674C>T | p.Pro225Leu[a](p.P225L) | 1 (1.4) |
| Total mutations | | 70 (100) |

[a] Novel mutations detected in this study.

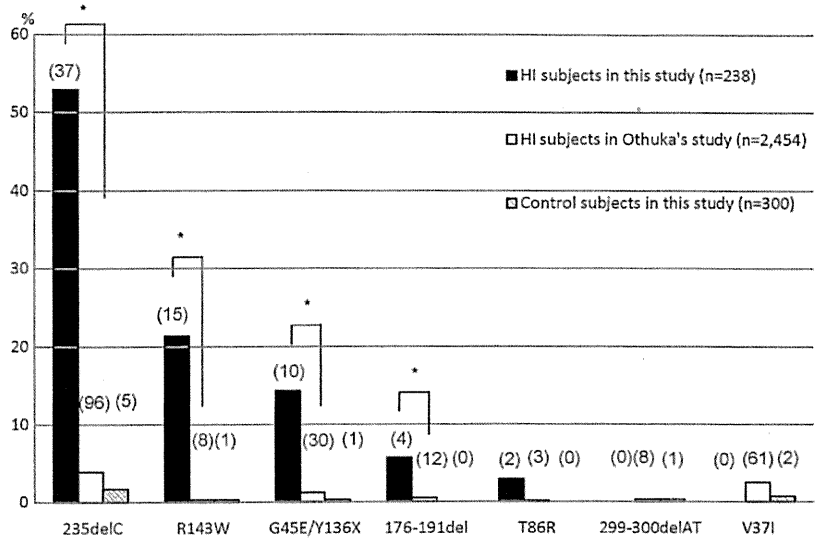


**Fig. 1.** Allele frequency for each mutation in three groups. A $Z$-test was used to assess the difference in frequency. Note the $P$-value of <0.01 between the two deafness groups for c.235delC, p.R143W, p.G45E/Y136X, and c.176-191del. $^{*}P < 0.01$.

(p.R32S and p.P225L) are highly conserved among various species, and we did not detect any of these mutations in 300 chromosomes in normal Japanese controls.

## 4. Discussion

In this study, *GJB2*-related deafness patients accounted for 29.4% of non-syndromic deafness cases. This frequency was less than in a previous report, which pointed to a frequency of around 50% [6]. Familial cases were twice as prevalent as sporadic cases. In most of the previously reported studies, the prevalence of *GJB2* mutations was significantly higher in familial non-syndromic deafness than in sporadic cases [7,26,27]. The frequent mutations of *GJB2* (c.235delC, p.R143W, p. G45E/Y136X, and c.176-191del) in this study were partly different from previous reports [25]. It is assumed that all of our subjects had severe to profound deafness, as they had received cochlear implants, whereas Ohtsuka's subjects had mild to profound deafness and included heterozygous mutations. A few studies have confirmed that some genotypes are correlated with clinical phenotypes in *GJB2*-related deafness. Further, truncating mutations are associated with a greater degree of deafness than non-truncating mutations [9,21,22]. For this reason, three of these cases might be truncating mutations. In contrast, p.R143W mutation was previously implicated in an extraordinarily high prevalence of profound deafness in Ghana [15,28] and Caucasians [9]. This missense mutation may also show an important correlation with severe deafness in Japan. On the other hand, an effect of geography on the allele frequency may have been present, because most of our subjects were from a different area compared to a previous report [25].

The relation between p.V37I mutation of *GJB2* and SNHL is controversial. While some reports suggest that this mutation is

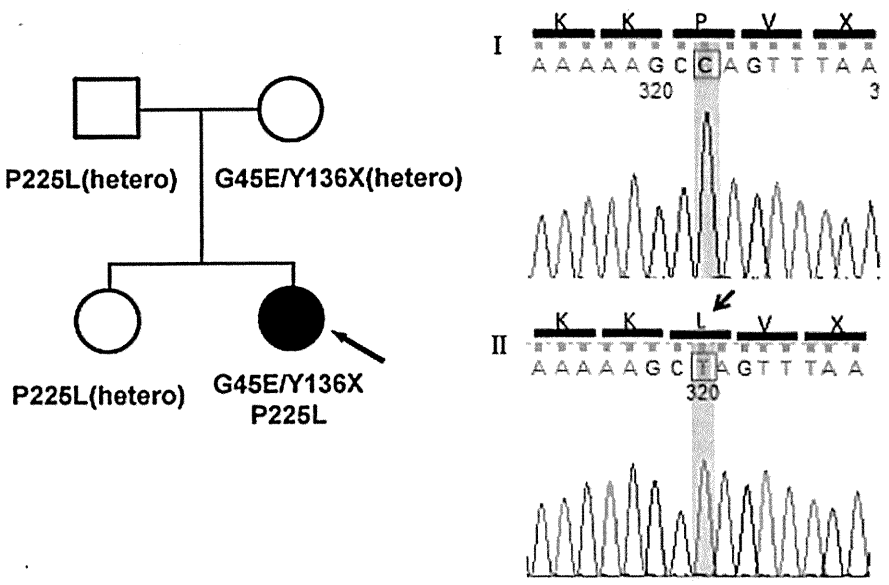


**Fig. 2.** (A) The pedigree and PCR direct sequencing results for the family; the arrow indicates the proband. (B) The sequencing results on TA cloning. Genomic PCR products were subcloned into a plasmid vector and sequenced separately (see Section 2). The sequences from independent clones are shown in the above two examples. I shows wild-type sequence, whereas II shows mutated sequence in which the proline residue is changed to leucine. Three of 8 subclones showed a missense mutation similar to that in II.

more common among individuals of Asian ancestry [11,12,29], others suggest that homozygous p.V37I is associated with slight/mild hearing loss [22,30,31]. In this study, no cases of homozygous p.V37I were observed. These findings support that this mutation is associated with mild hearing loss, because all of our subjects showed severe deafness.

The two unreported *GJB2* mutations, p.R32S and p.P225L, were not detected in normal hearing controls. These appeared in amino acid residues that were highly conserved. Additionally, three types of mutation were seen in arginine as the thirty-second amino acid, such as p.R32C, p.R32L, and p.R32H. Therefore, R32 is thought to be a mutation "hot spot." Thus, it is likely that these are pathological mutations, rather than rare or functionally neutral polymorphic changes. On the other hand, the mutation site of p.P225 located at the C-terminus of Connexin26 has not previously been reported. As the C-terminus region of connexins is thought to be an important region for intracellular molecular signaling and interaction with scaffolding proteins and the cytoskeleton [32–34], p.P225L mutation found in this study may affect important intracellular molecular networks to maintain the normal function of the cochlear gap junction.

## 5. Conclusion

In conclusion, this study identified significant genotypic features of Japanese children with profound non-syndromic deafness. Further research is required covering a broader range of genes in the subjects in this study with either single heterozygous or no mutation, in order to better understand the epidemiology of deafness in Japan.

## Acknowledgements

We thank all the subjects who participated in the present study. We also thank Ms. Naoko Tamura and Ms. Tomoko Kataoka (Tokyo Medical University School of Medicine), for recruiting families with non-syndromic deafness, and Ms. Junko Onoda (Juntendo University School of Medicine) for assisting in our experiments.

## References

[1] A.C. Davis, The prevalence of deafness and reported hearing disability among adults in Great Britain, Int. J. Epidemiol. 18 (1989) 911–917.
[2] D.H. Wilson, P.G. Walsh, L. Sanchez, The epidemiology of deafness in an Australian adult population, Int. J. Epidemiol. 28 (1999) 247–252.
[3] N.E. Morton, Genetic epidemiology of deafness, Ann. N. Y. Acad. Sci. 630 (1991) 1631.
[4] M.L. Marazita, L.M. Ploughman, B. Rawlings, E. Remington, K.S. Arnos, W.E. Nance, Genetic epidemiological studies of early-onset deafness in the U.S. school-age population, Am. J. Med. Genet. 46 (1993) 486–491.
[5] V. Kalatzis, C. Petit, The fundamental and medical impacts of recent progress in research on hereditary hearing loss, Hum. Mol. Genet. 7 (1998) 1589–1597.
[6] A. Kenneson, K. Van Naarden Braun, C. Boyle, GJB2 (connexin 26) variants and nonsyndromic sensorineural hearing loss: a HuGE review, Genet. Med. 4 (2002) 258–274.
[7] F. Denoyelle, S. Marlin, D. Weil, L. Moatti, P. Chauvin, E.N. Garabedian, et al., Clinical features of the prevalent form of childhood deafness, DFNB1, due to a connexin-26 gene defect: Implications for genetic counselling, Lancet 353 (1999) 1298–1303.
[8] A. Murgia, E. Orzan, R. Polli, M. Martella, C. Vinanzi, E. Leonardi, et al., Cx26 deafness: mutation analysis and clinical variability, J. Med. Genet. 36 (1999) 829–832.
[9] R.L. Snoeckx, P.L. Huygen, D. Feldmann, S. Marlin, F. Denoyelle, J. Waligora, et al., *GJB2* mutations and degree of hearing loss: a multicenter study, Am. J. Hum. Genet. 77 (2005) 945–957.
[10] Y. Fuse, K. Doi, T. Hasegawa, A. Sugii, H. Hibino, T. Kubo, Three novel connexin26 gene mutations in autosomal recessive non-syndromic deafnesss, Neuro Report 10 (1999) 1853–1857.
[11] S. Abe, S. Usami, H. Shinkawa, P.M. Kelley, W.J. Kimberling, Prevalent connexin 26 gene (*GJB2*) mutations in Japanese, J. Med. Genet. 37 (2000) 41–43.
[12] T. Kudo, K. Ikeda, S. Kure, Y. Matsubara, T. Oshima, K. Watanabe, et al., Novel mutations in the connexin 26 gene (*GJB2*) responsible for childhood deafness in the Japanese population, Am. J. Med. Genet. 90 (2000) 141–145.
[13] H.J. Park, S.H. Hahn, Y.M. Chun, K. Park, H.N. Kim, Connexin 26 mutations associated with nonsyndromic hearing loss, Laryngoscope 110 (2000) 1535–1538.
[14] P. Gasparini, R. Rabionet, G. Barbujani, S. Melchionda, M. Petersen, K. Brondum-Nielsen, et al., High carrier frequency of the 35delG deafness mutation in European populations, Genetic Analysis Consortium of GJB2 35delG, Eur. J. Hum. Genet. 8 (2000) 19–23.
[15] G.W. Brobby, B. Muller-Myhsok, R.D. Horstmann, Connexin 26 R143W mutation associated with recessive nonsyndromic sensorineural deafness in Africa, N. Engl. J. Med. 338 (1998) 548–550.
[16] M. Maheshwari, R. Vijaya, M. Ghosh, S. Shastri, M. Kabra, P.S. Menon, Screening of families with autosomal recessive non-syndromic hearing impairment (ARNSHI) for mutations in GJB2 gene: Indian scenario, Am. J. Med. Genet. A 120A (2003) 180–184.
[17] M. RamShankar, S. Girirajan, O. Dagan, H.M. Ravi Shankar, R. Jalvi, R. Rangasayee, et al., Contribution of connexin26 (GJB2) mutations and founder effect to non-syndromic hearing loss in India, J. Med. Genet. 40 (2003) e68.
[18] G. Minárik, V. Ferák, E. Feráková, A. Ficek, H. Poláková, L. Kádasi, High frequency of GJB2 mutation W24X among Slovak Romany (Gypsy) patients with non-syndromic hearing loss (NSHL), Gen. Physiol. Biophys. 22 (2003) 549–556.
[19] P. Seeman, M. Malíková, D. Rasková, O. Bendová, D. Groh, M. Kubálková, et al., Spectrum and frequencies of mutations in the GJB2 (Cx26) gene among 156 Czech patients with pre-lingual deafness, Clin. Genet. 66 (2004) 152–157.
[20] A. Alvarez, I. del Castillo, M. Villamar, L.A. Aguirre, A. González-Neira, A. López-Nevot, et al., High prevalence of the W24X mutation in the gene encoding connexin-26 (GJB2) in Spanish Romani (gypsies) with autosomal recessive non-syndromic hearing loss, Am. J. Med. Genet. A 137A (2005) 255–258.
[21] K. Cryns, E. Orzan, A. Murgia, P.L. Huygen, F. Moreno, I. del Castillo, et al., A genotype-phenotype correlation for *GJB2* (connexin 26) deafness, J. Med. Genet. 41 (2004) 147–154.
[22] T. Oguchi, A. Ohtsuka, S. Hashimoto, A. Oshima, S. Abe, Y. Kobayashi, et al., Clinical features of patients with *GJB2* (connexin 26) mutations: Severity of hearing loss is correlated with genotypes and protein expression patterns, J. Hum. Genet. 50 (2005) 76–83.
[23] K. Fukushima, K. Sugata, N. Kasai, S. Fukuda, R. Nagayasu, N. Toida, et al., Better speech performance in cochlear implant patients with GJB2-related deafness, Int. J. Pediatr. Otorhinolaryngol. 62 (2002) 151–157.
[24] F.J. Del Castillo, M. Rodriguez-Ballesteros, A. Alvarez, T. Hutchin, E. Leonardi, C.A. de Oliveira, et al., A novel deletion involving the connexin-30 gene, del(*GJB6*-d13s1854), found in trans with mutations in the *GJB2* gene (connexin-26) in subjects with DFNB1 non-syndromic deafnesss, J. Med. Genet. 42 (2005) 588–594.
[25] A. Ohtsuka, I. Yuge, S. Kimura, A. Namba, S. Abe, L. Van Laer, et al., *GJB2* deafness gene shows a specific spectrum of mutations in Japan, including a frequent founder mutation, Hum. Genet. 112 (2003) 329–333.
[26] J. Loffler, D. Nekahm, A. Hirst-Stadlmann, B. Gunther, H.J. Menzel, G. Utermann, et al., Sensorineural hearing loss and the incidence of Cx26 mutations in Austria, Eur. J. Hum. Genet. 9 (2001) 226–230.
[27] A. Pampanos, J. Economides, V. Iliadou, P. Neou, P. Leotsakos, N. Voyiatzis, et al., Prevalence of *GJB2* mutations in prelingual deafness in the Greek population, Int. J. Pediatr. Otorhinolaryngol. 65 (2002) 101–108.
[28] C. Hamelmann, G.K. Amedofu, K. Albrecht, B. Muntau, A. Gelhaus, G.W. Brobby, et al., Pattern of connexin 26 (*GJB2*) mutations causing sensorineural deafness in Ghana, Hum. Mutat. 18 (2001) 84–85.
[29] WangYC, C.Y. Kung, M.C. Su, C.C. Su, H.M. Hsu, C.C. Tsai, et al., Mutations of Cx26 gene (*GJB2*) for prelingual deafness in Taiwan, Eur. J. Hum. Genet. 10 (2002) 495–498.
[30] C. Huculak, H. Bruyere, T.N. Nelson, F.K. Kozak, S. Langlois, V37I connexin 26 allele in patients with sensorineural hearing loss: Evidence of its pathogenicity, Am. J. Med. Genet. A 140 (2006) 2394–2400.
[31] H.H. Dahl, K. Saunders, T.M. Kelly, A.H. Osborn, S. Wilcox, B. Cone-Wesson, et al., Prevalence and nature of connexin 26 mutations in children with non-syndromic deafnesss, Med. J. Aust. 175 (2001) 191–194.
[32] L.A. Elias, D.D. Wang, A.R. Kriegstein, Gap junction adhesion is necessary for radial migration in the neocortex, Nature 448 (2007) 901–907.
[33] P.E. Martin, G. Blundell, S. Ahmad, R.J. Errington, W.H. Evans, Multiple pathways in the trafficking and assembly of connexin 26, 32 and 43 into gap junction intercellular communication channels, J. Cell Sci. 114 (2001) 3845–3855.
[34] K.A. Schalper, N. Palacios-Prado, M.A. Retamal, K.F. Shoji, A.D. Martínez, J.C. Sáez, Connexin hemichannel composition determines the FGF-1-induced membrane permeability and free $[Ca^{2+}]i$ responses, Mol. Biol. Cell 19 (2008) 3501–3513.

INTERNATIONAL JOURNAL OF Experimental Pathology

*Int. J. Exp. Path.* (2010)

ORIGINAL ARTICLE

# Analysis of subcellular localization of Myo7a, Pcdh15 and Sans in *Ush1c* knockout mice

Denise Yan[1], Kazusaku Kamiya[1], Xiao Mei Ouyang and Xue Zhong Liu

*Department of Otolaryngology, University of Miami, Miami, FL, USA*

INTERNATIONAL JOURNAL OF EXPERIMENTAL PATHOLOGY

doi: 10.1111/j.1365-2613.2010.00751.x

Received for publication:
30 June 2010
Accepted for publication:
21 October 2010

**Correspondence:**
Dr Xue Zhong Liu
Department of Otolaryngology (D-48)
University of Miami
1666 NW 12th Avenue
Miami, FL 33136
USA
Tel.: 305 243 5695
Fax: 305 243 4925
E-mail: xliu@med.miami.edu

[1]These authors contributed equally to this work.

## Summary

Usher syndrome (USH) is the most frequent cause of combined deaf-blindness in man. An important finding from mouse models and molecular studies is that the USH proteins are integrated into a protein network that regulates inner ear morphogenesis. To understand further the function of harmonin in the pathogenesis of USH1, we have generated a targeted null mutation *Ush1c* mouse model. Here, we examine the effects of null mutation of the *Ush1c* gene on subcellular localization of Myo7a, Pcdh15 and Sans in the inner ear. Morphology and proteins distributions were analysed in cochlear sections and whole mount preparations from $Ush1c^{-/-}$ and $Ush1c^{-/+}$ controls mice. We observed the same distribution of Myo7a throughout the cytoplasm in knockout and control mice. However, we detected Pcdh15 at the base of stereocilia and in the cuticular plate in cochlear hair cells from $Ush1c^{+/-}$ controls, whereas in the knockout $Ush1c^{-/-}$ mice, Pcdh15 staining was concentrated in the apical region of the outer hair cells and no defined staining was detected at the base of stereocilia nor in the cuticular plate. We showed localization of Sans in the stereocilia of controls mouse cochlear hair cells. However, in cochleae from $Ush1c^{-/-}$ mice, strong Sans signals were detected towards the base of stereocilia close to their insertion point into the cuticular plate. Our data indicate that the disassembly of the USH1 network caused by absence of harmonin may have led to the mis-localization of the Protocadherin 15 and Sans proteins in the cochlear hair cells of $Ush1c^{-/-}$ knockout mice.

**Keywords**
deafness, inner ear, knockout mouse, Usher 1C, Usher syndrome

## Introduction

Usher syndrome (USH) is an autosomal recessive disorder characterized by congenital hearing loss and progressive retinal degradation leading to gradual loss of the visual field and blindness.

Three major clinical subtypes (USH type I, USH type II and USH type III) are distinguished on the basis of differences in the severity of the hearing loss, the presence or absence of vestibular dysfunction and the age of onset of retinitis pigmentosa (RP) (Smith *et al.* 1994). In USH type 1, the hearing loss is profound and vestibular function is absent. The onset of progressive RP is before puberty. Usher syndrome type 2 is associated with less severe deafness, normal vestibular function and onset of RP during or after puberty. Usher syndrome type 3 patients also have milder deafness, but, unlike in USH2, the hearing loss is progressive, there is variable impairment of vestibular function and late-onset RP. Each USH subtype is genetically heterogeneous. To date, seven USH1 loci (USH1B-USH1H) have been identified by linkage analyses of USH1 families. Five of the corresponding genes have been cloned: the actin-based motor protein myosin VIIa (*Myo7a, USH1B*) (Gibson *et al.* 1995; Weil *et al.* 1995); two cadherin-related proteins, otocadherin or Cadherin 23 (*Cdh23, USH1D*) (Bolz *et al.* 2001; Bork *et al.* 2001) and Protocadherin 15 (*Pcdh15, USH1F*) (Ahmed *et al.* 2001; Alagramam *et al.* 2001a); and two scaffold proteins, harmonin (*USH1C*) (Verpy *et al.* 2000; Bitner-Glindzicz *et al.* 2000) and Sans (*USH1G*) (Kikkawa *et al.* 2003; Weil *et al.* 2003). The USH proteins are involved in hair bundle morphogenesis in the inner ear by means of protein–protein interactions. In a combination of cell cotransfection

and *in vitro* binding assays, harmonin has been shown to bind to any of the other USH proteins (El-Amraoui & Petit 2005; Yan & Liu 2010; Zheng *et al.* 2010).

A mouse mutant has been reported for each of the known *Ush1* genes; shaker1 (*sh1*) for *Myo7a* (Gibson *et al.* 1995), waltzer (*v*) for *Cdh23* (Di Palma *et al.* 2001; Wilson *et al.* 2001), Ames waltzer (*av*) for *Pcdh15* (Alagramam *et al.* 2001b), deaf circler (*dfcr*) and targeted mouse models for *Ush1c* (Johnson *et al.* 2003; Lentz *et al.* 2007; Lefevre *et al.* 2008; Tian *et al.* 2010) and Jackson shaker (*js*) for *Ush1g* (Kikkawa *et al.* 2003). All of these mice are deaf, exhibit vestibular dysfunction and display similar morphological abnormalities in hair bundle development. In all of these models, the hair cell stereocilia vary irregularly in height and splay out from one another indicating defective lateral interactions. Investigations into the localization of the USH proteins within the developing stereocilia in mice, combined with *in vitro* studies to determine the various interactions between the constituent molecules, have revealed an 'Usher interactome' that is responsible for bundle cohesion. Some of the Ush1 mutant mice (*sh1*, *v*, *av*) exhibited electroretinogram anomalies (Libby & Steel 2001), a defective retinal pigment epithelium has been described in *sh1* mice (Gibbs *et al.* 2003, 2004) and retinal degeneration has been reported in *Ush1c216AA* knockin-in mice (Lentz *et al.* 2010).

The gene encoding harmonin consists of 28 coding exons, alternative splicing of which leads to 10 USH1C isoforms. These alternative transcripts form three subclasses (a, b and c) depending on the domain composition of the protein. The isoform 'a' transcript subclass is expressed ubiquitously in many tissues, whereas the longest 'b' transcript is restricted largely to the inner ear. The short isoform 'c' has a much broader tissue distribution. The harmonin isoforms differ in the number of protein–protein interaction domains (PDZ, postsynaptic density/disc-large/zonal occludens 1), coiled–coiled domains (CC) and the presence of a proline-serine-threonine-rich domain (Verpy *et al.* 2000). Deaf circler, *dfcr* and *dfcr-2J* spontaneous mutant mice have been described as models for human *USH1C*. The mutant *dfcr* is defective in all harmonin isoforms (a, b and c). Only the harmonin b isoform subclass is affected by the *dfcr-2J* mutation (Johnson *et al.* 2003). However, altered harmonin isoforms may retain partial function because the normal reading frame of the *Ush1c* transcripts is not changed in the shortened *dfcr* transcripts of either isoform a or isoform b. Furthermore, none of the three PDZ-encoding domains are deleted in *dfcr* mutant transcripts. Both a USH1C knockin and knockout mouse have also been reported (Lentz *et al.* 2007; Lefevre *et al.* 2008). To further understand the role of harmonin in the pathogenesis that leads to USH1, we have recently generated a targeted null mutation *Ush1c* mouse model in which the first four exons of the *Usher 1c* gene have been replaced by a reporter gene (Liu *et al.* 2005; Yan *et al.* 2006; Tian *et al.* 2010). Our model is unique because none of the previous targeted mouse models for USH1C include a reporter gene in the construct to facilitate expression analysis in various tissues. Here, we examine the effects of *Ush1c* mutation on spatial subcellular localization of Myo7a, Pcdh15 and Sans proteins in the inner ear. In whole mount of inner ears from mutant, Myo7a was not affected at the timepoint we analysed the mutant mice, although it is a critical part of the USH interactome. However, we found both Pcdh15 and Sans displayed an altered localization in the mutant mice that may have resulted from disruption of the entire USH1 complex.

## Materials and methods

Inner ears isolated from the $Ush1c^{-/-}$ and$^{+/-}$ mice at postnatal day 21 (PD21) were fixed by immersion in 4% paraformaldehyde (pH 7.4) for 2-5 h at 4°C. The organ of Corti was dissected from the cochlear spiral in phosphate-buffered saline (PBS) using a fine needle. Samples were then permeabilized in 0.5% Triton X-100 for 30 min, then washed in PBS. Non-specific binding sites were blocked using 5% normal goat serum (Life Technologies, Gaithersburg, MD, USA) and 2% bovine serum albumin (ICN, Aurora, OH, USA) in PBS for 2 h. Samples were incubated for 2 h in the primary antibodies at 5 μg/ml in blocking solution. After several rinses in PBS, samples were incubated in Alexa Fluor 488-conjugated anti-rabbit IgG goat at 1:400 (Molecular Probes, Eugene, OR, USA) for 40 min. Samples were mounted using a ProLong Antifade kit (Molecular Probes) and analysed with a laser scanning confocal microscope (LSM-510; Zeiss, Thornwood, NY, USA). The polyclonal antibody against Myo7a (ab3481) was obtained from Abcam (Cambridge, MA, USA). The anti-PCDH15 antibody was generated against a mixed peptide sequence corresponding to amino acid 24-37 (SWGQYDDDWQYEDC) and amino acid 1847-1860 (C+TFTTQPPASNPQWG), and the anti-USH1G antibody was against the central portion of the Sans protein (amino acid 354-372).

## Results

Homozygous mutant mice ($Ush1c^{-/-}$) exhibit the abnormal behaviour (circling and/head-tossing) that are typical of mice with profound hearing loss and vestibular dysfunction. $Ush1c^{-/-}$ mice were completely deaf, as there was no detectable auditory-evoked brainstem response (ABR) with 100 dB SPL stimuli, whereas age-matched $Ush1c^{+/-}$ controls showed ABR thresholds in the normal hearing-range at PD15 and PD22. Examination of hair cell surface preparations by scanning electron microscopy from birth (PD0) to PD120 in $Ush1c^{-/-}$ showed progressively disorganized outer hair cell (OHC) stereocilia compared with the well-organized pattern and rigid structure typical of normal stereocilia. Stereocilia of inner hair cells (IHCs) of mutant mice also exhibited a disorganized appearance, but to a lesser degree than did the OHCs (Tian *et al.* 2010).

To address the possibility that absence of harmonin disrupts the USH1 protein complex, we analysed in this study the distribution of Myosin VIIa protein in whole mounts, and of Protocadherin 15 and Sans in cross sections, of inner

ears from *Ush1c*$^{-/-}$ mice. Light microscopy examinations of sections through apical regions of the cochleae of *Ush1c*$^{-/-}$ at PD2 revealed no apparent hair cell degeneration (data not shown). However, in cochlear whole mounts from *Ush1c*$^{-/-}$ mice at PD21, some gaps are seen in the regular array of hair cells. Although the single row of IHCs and the three rows of OHCs can be distinguished by surface scanning of the hair cells (Figure 1b), fragmentation of the OHC stereociliary bundles into two clumps was observed, instead of an integral, single 'V'-shaped bundle as in wild-type hair cells (Figure 1d, arrow). This fragmented aspect was not detected in stereocilia of IHCs at this timepoint (IHC; Figure 1b), suggesting that they were beginning to degenerate. However, confocal microscopic analysis of the hair cells in the basal layer revealed structural morphological abnormalities in both OHCs and IHCs, with a more disorganized appearance in IHC (Figure 1f). Scanning electron microscopy of *Ush1c*$^{-/-}$ mice from PD21 to PD120 showed a progressive degeneration of the hair cells and stereocilia of the cochlea (Tian *et al.* 2010). Myosin 7a has previously been shown to be expressed within the stereocilia and within the cuticular plate, which anchors the base of each stereocilium. In the present study, Myosin 7a was distributed throughout the cytoplasm in *Ush1c*$^{-/-}$ and control mice in the labelled hair cells, revealing structural morphological abnormalities characterized by disorganized, misaligned inner and OHCs (Figure 1e, f).

In cochlear hair cells from heterozygous *Ush1c*$^{+/-}$ control mice, we detected Protocadherin 15 at the base of stereocilia and in the cuticular plate (as shown by the arrow in Figure 2c), whereas in the mutant *Ush1c*$^{-/-}$, Protocadherin 15 immunoreactivity was found accumulated in the apical region of the OHC and no defined staining was detected at the base of stereocilia and little Pcdh15 expression was present at the cuticular plate (Figure 2d). Likewise, in the knockout mice, Sans was undetectable in the stereocilia bundles of cochlear hair cells at PD21 (Figures 3b, d), in contrast to the heterozygous controls (*Ush1c*$^{+/-}$, Figure 3c). Instead, strong Sans staining was observed towards the base of stereocilia close to their insertion point into the cuticular plate with a slight staining of the cytoplasmic region of OHC in cochleae from *Ush1c*$^{-/-}$ mice (Figure 3d). These results suggest a mis-localization of the Pcdh15 and Sans proteins in

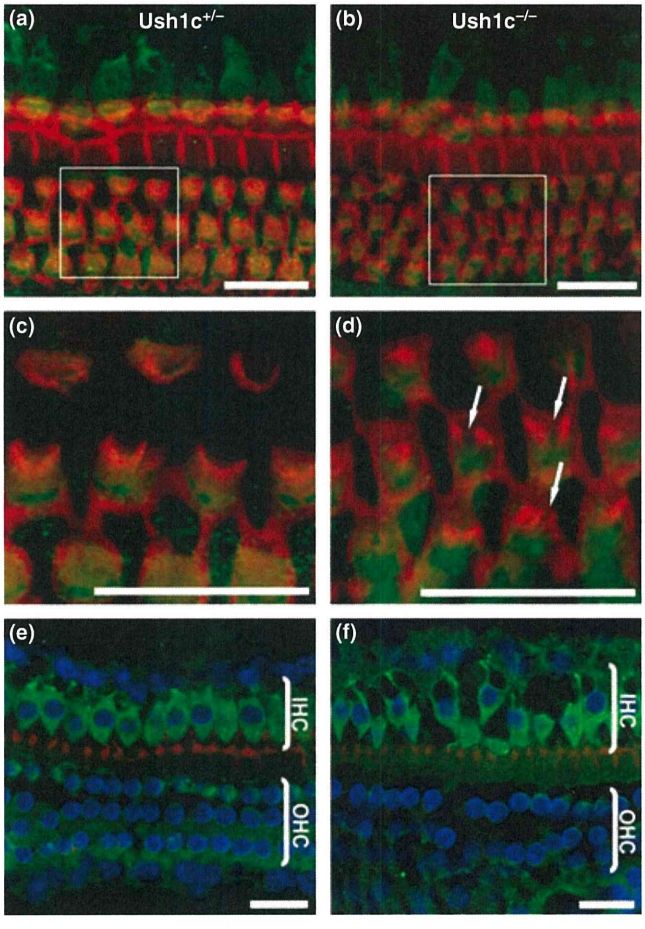


**Figure 1** Abnormalities at the apical surface of outer hair cells (OHC) and structural defects of the hair cells in *Ush1c*$^{-/-}$ mice at PD21. Cochlear whole mounts were stained with phalloidin (red) to reveal F-actin in stereocilia and an antibody against myosin 7a (green) to show the basal structure of the hair cells in *Ush1c*$^{+/-}$ (a, c and e) and *Ush1c*$^{-/-}$ mice (b, d and f). Stereocilia defects were observed in the middle part of the stereocilia bundles of the OHCs (d, arrows) that were not detected in stereocilia of inner hair cells (IHC; b). c and d show magnified images corresponding to the boxed areas in a and b respectively. The confocal analysis at the basal level of hair cells with nuclear staining (e and f) (DAPI, Blue). Bars = 20 μm.

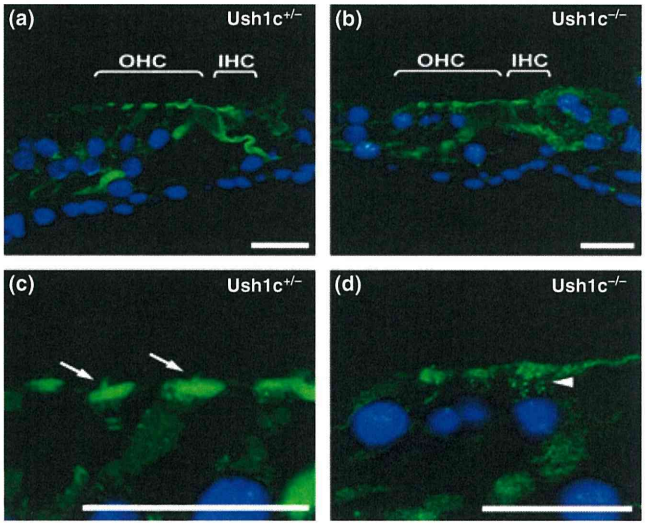


**Figure 2** Localization of Protocadherin 15 (green) in the cochlear hair cells of *Ush1c*-knockout mice at PD21. Cross sections of the organ of Corti were stained with an antibody to Protocadherin 15 (green). In *Ush1c*$^{+/-}$ mice (a and c), expression of Protocadherin 15 was localized at the base of stereocilia (left panel, arrow) and in the cuticular plate. In contrast, in *Ush1c*$^{-/-}$ mice (b and d), Protocadherin 15 immunoreactivity appears (arrowhead) diffuse above nuclei (DAPI-Blue). Bars = 20 μm.

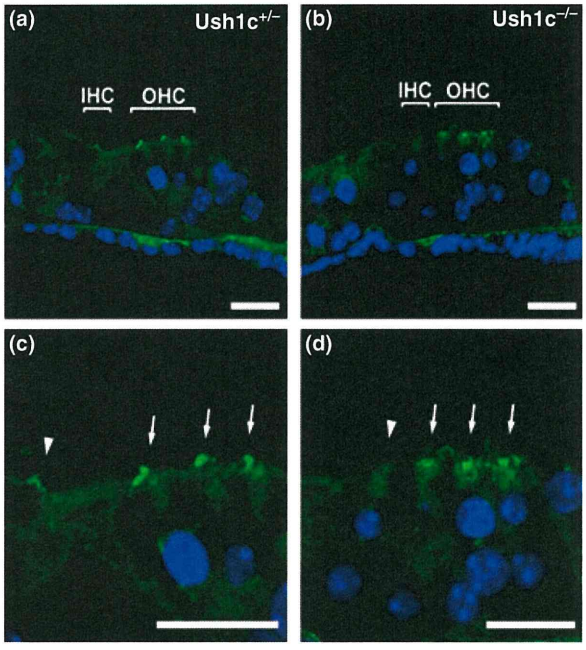


**Figure 3** Localization of Sans (green) in the cochlear hair cells of *Ush1c*$^{-/-}$ mice at PD21. Cross sections of the organ of Corti of *Ush1c*$^{+/-}$ (a and c) and *Ush1c*$^{-/-}$ (b and d) mice were stained with an antibody to Sans (green). c and d are higher magnification images of a and b respectively. Arrowheads and arrows indicate inner hair cells and outer hair cells (OHC) respectively. Nuclei were stained by DAPI (Blue). Sans was localized in the stereocilia bundles in *Ush1c*$^{+/-}$ cochlear hair cells at PD21 (c). However, in *Ush1c*$^{-/-}$ mice, strong signals were observed towards the base of stereocilia close to their insertion into the cuticular plate with a slight cytoplasmic staining of OHC (d). Bars indicate 20 μm.

*Ush1c*$^{-/-}$ mice, characterized by a shift of the immunoreactivity of the proteins towards the base of stereocilia.

## Discussion

The USH gene products are part of a protein complex in hair cells of the inner ear. The actin-bundling and PDZ-domain-containing protein harmonin may coordinate the activities of the USH proteins and bridge them to the cytoskeleton of the hair cell (Boeda *et al.* 2002). Disruption of the USH protein network leads to stereociliary disorganization, as observed in mouse models, and is thought to be responsible for congenital deafness in patients with USH (Petit 2001).

Mouse models for USH have played a crucial role in identifying defective genes responsible for USH1 in humans and furthering our understanding of the function of USH1 proteins in normal and disease conditions. All mouse USH1 models are deaf and exhibit vestibular dysfunction. In these mutants, the sensory cells of the cochlea display anomalies in hair bundle development, indicating an essential function for USH1 proteins in stereocilia differentiation (El-Amraoui & Petit 2005). The abnormal stereocilia morphology observed in our *Ush1c* knockout mice is similar to that reported in mouse models for other forms of human USH1.

Regarding spatiotemporal expression, immunohistochemical studies show that the USH1 proteins are expressed in hair cells of the inner ear throughout life. However, USH1 protein subcellular distribution in the stereocilia varies dramatically during development until maturity is reached. Expression of harmonin, Cdh23 and Pcdh15 is detectable in the hair bundle from the moment the bundle emerges at the apical surface of sensory hair cells (Boeda *et al.* 2002; Ahmed *et al.* 2003). Harmonin b is found concentrated at the tips of stereocilia during early postnatal stages but its expression diminishes around PD30 in both the cochlea and vestibule (Boeda *et al.* 2002). The spatiotemporal expression pattern of Cdh23 parallels that of harmonin b, being first observed along the entire length of the emerging stereocilia and then restricted to the tip region.

Notably, Grillet *et al.* (2009) have recently shown that harmonin b is a component of the upper tip-link density, where CDH23 inserts into the stereociliary membrane and is required for normal hair cell mechanoelectrical transduction. In foetal cochlea, Pcdh15 can be detected in supporting cells, outer sulcus cells and the spiral ganglion (Alagramam *et al.* 2001b), while in the mature inner ear, Pcdh15 is also localized in stereocilia of sensory hair cells of both the cochlea and the vestibular organ (Ahmed *et al.* 2003). CDH23 and PCDH15 have been shown to be present in the transient lateral stereocilial and kinocilial links and that the two cadherin proteins interact to form tip-link filaments in sensory hair cells (Sollner *et al.* 2004; Michel *et al.* 2005; Kazmierczak *et al.* 2007). MYO7A is expressed in the mechanosensory hair cells of the vestibular organ and cochlea where it is predominantly localized in the stereocilia, but is also detected within the cuticular plate and the pericuticular necklace region, which is characterized by a dense ring of vesicles (El-Amraoui *et al.* 1996; Hasson *et al.* 1997; Boeda *et al.* 2002).

In this study, we investigated the effect of the *Ush1c* knockout mice on subcellular expression of Myosin 7a, Pcdh15 and Sans in the inner ear. We observed the same distribution of Myosin 7a expression throughout the cytoplasm in knockout and control mice which may indicate that Myosin 7a is expressed earlier than harmonin. This may also suggest that Myosin 7a does not rely on the presence of harmonin isoforms for its cytoplasmic distribution. Whether the cytoplasmic Myosin 7a requires harmonin for hair cells function, however, remains to be examined. We detected Pcdh15 at the base of stereocilia and in the cuticular plate in cochlear hair cells from *Ush1c*$^{+/-}$ controls, whereas in the mutant *Ush1c*$^{-/-}$, Pcdh15 immunoreactivity was found accumulated in the apical region of the OHC and no defined staining was detected at the base of stereocilia nor in the cuticular plate. The scaffold protein Sans has previously been shown localized in the apical hair cell bodies underneath the cuticular plate of cochlear and vestibular hair cells of PD3 mice (Adato *et al.* 2005), but not in the stereocilia. Using an antibody against a peptide sequence corresponding

to the central portion of Sans (amino acid 354–372), we found the protein localized in the stereocilia bundles of mouse cochlear hair cells at PD21 in controls mouse. However, in cochleae from *Ush1c*$^{-/-}$ mice, strong Sans signals were observed towards the base of stereocilia close to their insertion point into the cuticular plate with a slight staining of the cytoplasmic region of OHC. Overall, our data indicated that in mice deficient in harmonin, both interacting partners Pcdh15 and Sans are mislocalized. The epitopes recognized by our antibodies against Pcdh15 and Sans were shifted towards the basal body of the hair cells, whereas they are expressed in the stereocilia of normal control mice.

## Acknowledgements

The work is supported by NIH DC05575. We thank Qing Y Zheng for providing *Ush1c* knockout mice DC007392.

## References

Adato A., Michel V., Kikkawa Y. *et al.* (2005) Interactions in the network of Usher syndrome type 1 proteins. *Hum. Mol. Genet.* **14**, 347–356.

Ahmed Z.M., Riazuddin S., Bernstein S.L. *et al.* (2001) Mutations of the protocadherin gene pcdh15 cause usher syndrome type 1F. *Am. J. Hum. Genet.* **69**, 25–34.

Ahmed Z.M., Riazuddin S., Riazuddin S., Wilcox E.R. (2003) The molecular genetics of Usher syndrome. *Clin. Genet.* **63**, 431–444.

Alagramam K.N., Yuan H., Kuehn M.H., Murcia C.L., Wayne S., Srisailpathy C.R. (2001a) Mutations in the novel protocadherin pcdh15 cause usher syndrome type 1f. *Hum. Mol. Genet.* **10**, 1709–1718.

Alagramam K.N., Murcia C.L., Kwon H.Y., Pawlowski K.S., Wright C.G., Woychik R.P. (2001b) The mouse ames waltzer hearing-loss mutant is caused by mutation of pcdh15, a novel protocadherin gene. *Nat. Genet.* **27**, 99–102.

Bitner-Glindzicz M., Lindley K.J., Rutland P. *et al.* (2000) A recessive contiguous gene deletion causing infantile hyperinsulinism, enteropathy and deafness identifies the usher type 1c gene. *Nat. Genet.* **26**, 56–60.

Boeda B., El-Amraoui A., Bahloul A. *et al.* (2002) Myosin VIIa, harmonin and cadherin 23, three Usher I gene products that cooperate to shape the sensory hair cell bundle. *EMBO J.* **21**, 6689–6699.

Bolz H., von Brederlow B., Ramírez A. *et al.* (2001) Mutation of CDH23, encoding a new member of the cadherin gene family, causes Usher syndrome type 1D. *Nat. Genet.* **27**, 108–112.

Bork J.M., Peters L.M., Riazuddin S. *et al.* (2001) Usher syndrome 1D and nonsyndromic autosomal recessive deafness DFNB12 are caused by allelic mutations of the novel cadherin-like gene CDH23. *Am. J. Hum. Genet.* **68**, 26–37.

Di Palma F., Holme R.H., Bryda E.C. *et al.* (2001) Mutations in cdh23, encoding a new type of cadherin, cause stereocilia disorganization in waltzer, the mouse model for usher syndrome type 1d. *Nat. Genet.* **27**, 103–107.

El-Amraoui A., Petit C. (2005) Usher I syndrome: unravelling the mechanisms that underlie the cohesion of the growing hair bundle in inner ear sensory cells. *J. Cell Sci.* **118**, 4593–4603.

El-Amraoui A., Sahly I., Picaud S., Sahel J., Abitbol M., Petit C. (1996) Human Usher 1B/mouse shaker-1: the retinal phenotype discrepancy explained by the presence/absence of myosin VIIA in the photoreceptor cells. *Hum. Mol. Genet.* **5**, 1171–1178.

Gibbs D., Kitamoto J., Williams D.S. (2003) Abnormal phagocytosis by retinal pigmented epithelium that lacks myosin VIIa, the Usher syndrome 1B protein. *Proc. Natl Acad. Sci. USA* **100**, 6481–6486.

Gibbs D., Azarian S.M., Lillo C. *et al.* (2004) Role of myosin VIIa and Rab27a in the motility and localization of RPE melanosomes. *J. Cell Sci.* **117**, 6473–6483.

Gibson F., Walsh J., Mburu P. *et al.* (1995) A type VII myosin encoded by the mouse deafness gene shaker-1. *Nature* **374**, 62–64.

Grillet N., Xiong W., Reynolds A. *et al.* (2009) Harmonin mutations cause mechanotransduction defects in cochlear hair cells. *Neuron* **62**, 375–387.

Hasson T., Gillespie P.G., Garcia J.A. *et al.* (1997) Unconventional myosins in inner-ear sensory epithelia. *J. Cell Biol.* **137**, 1287–1307.

Johnson K.R., Gagnon L.H., Webb L.S. *et al.* (2003) Mouse models of ush1c and dfnb18: phenotypic and molecular analyses of two new spontaneous mutations of the ush1c gene. *Hum. Mol. Genet.* **12**, 3075–3086.

Kazmierczak P., Sakaguchi H., Tokita J. *et al.* (2007) Cadherin 23 and protocadherin 15 interact to form tip-link filaments in sensory hair cells. *Nature* **6**, 449.

Kikkawa Y., Shitara H., Wakana S. *et al.* (2003) Mutations in a new scaffold protein sans cause deafness in jackson shaker mice. *Hum. Mol. Genet.* **12**, 453–461.

Lefevre G., Michel V., Weil D. *et al.* (2008) A core cochlear phenotype in ush1 mouse mutants implicates fibrous links of the hair bundle in its cohesion, orientation and differential growth. *Development* **135**, 1427–1437.

Lentz J., Pan F., Ng S.S., Deininger P., Keats B.J. (2007) Ush1c216a knock-in mouse survives katrina. *Mutat. Res.* **616**, 139–144.

Lentz J.J., Gordon W.C., Farris H.E. *et al.* (2010) Deafness and retinal degeneration in a novel USH1C knock-in mouse model. *Dev. Neurobiol.* **70**, 253–267.

Libby R.T., Steel K.P. (2001) Electroretinographic anomalies in mice with mutations in Myo7a, the gene involved in human Usher syndrome type 1B. *Invest. Ophthalmol. Vis. Sci.* **42**, 770–778.

Liu X.Z., Zheng Q.Y., Ouyang X.M., Du L.L., Johnson K.R., Yan D. (2005) Gene targeting and homologous recombination for USH1C gene. *Association for Research in Otolaryngology Meeting*. New Orleans, LA: The Fairmont February, 19–24.

Michel V., Goodyear R.J., Weil D. *et al.* (2005) Cadherin 23 is a component of the transient lateral links in the developing hair bundles of cochlear sensory cells. *Dev. Biol.* **280**, 281–294.

Petit C. (2001) Usher syndrome: from genetics to pathogenesis. *Annu. Rev. Genomics Hum. Genet.* **2**, 271–297.

Smith R.J., Berlin C.I., Hejtmancik J.F. *et al.* (1994) Clinical diagnosis of the Usher syndromes. Usher Syndrome Consortium. *Am. J. Med. Genet.* **50**, 32–38.

Sollner C., Rauch G.J., Siemens J. *et al.* (2004) Mutations in cadherin 23 affect tip links in zebrafish sensory hair cells. *Nature* **428**, 955–959.

Tian C., Liu X.Z., Han F. *et al.* (2010) Ush1c gene expression levels in the ear and eye suggest different roles for Ush1c in neurosensory organs in a new Ush1c knockout mouse. *Brain Res.* **1328**, 57–70.

Verpy E., Leibovici M., Zwaenepoel I. *et al.* (2000) A defect in harmonin, a PDZ domain-containing protein expressed in the inner ear sensory hair cells, underlies usher syndrome type 1C. *Nat. Genet.* **26**, 51–55.

Weil D., Blanchard S., Kaplan J. *et al.* (1995) Defective myosin viia gene responsible for usher syndrome type 1b. *Nature* **374**, 60–61.

Weil D., El-Amraoui A., Masmoudi S. *et al.* (2003) Usher syndrome type 1G (USH1G) is caused by mutations in the gene encoding sans, a protein that associates with the ush1c protein, harmonin. *Hum. Mol. Genet.* **12**, 463–471.

Wilson S.M., Householder D.B., Coppola V. *et al.* (2001) Mutations in cdh23 cause nonsyndromic hearing loss in waltzer mice. *Genomics* **74**, 228–233.

Yan D., Liu X.Z. (2010) Genetics and pathological mechanisms of Usher syndrome. *J. Hum.Genet.* **55**, 327–335.

Yan D., Zheng Q.Y., Ouyang X.M. *et al.* (2006) A gene knockout mouse model for Usher syndrome type 1C. *Association for Research in Otolaryngology Meeting*. Baltimore, February 2006.

Zheng L., Zheng J., Whitlon D.S., García-Añoveros J., Bartles J.R. (2010) Targeting of the hair cell proteins cadherin 23, harmonin, myosin XVa, espin, and prestin in an epithelial cell model. *J. Neurosci.* **30**, 7187–7201.